第百十三號

(昭和九年十月發行)

# 抄錄

# 切り缺きが翼の空氣力學的特性に及ぼす影響に關する實驗研究

工學士　岡　本　哲　史

本論文は 1932年の秋より 1934年の夏迄の二年間に行へる研究(1) のうち實驗研究の部分を纒めたものである．後縁に矩形の切り缺きを有する翼に就いて，之を更に翼幅方向に切り缺きを擴大した場合と翼弦方向に切り缺きを擴大した場合に分け，切り缺きが翼の性能に及ぼす影響を系統的に實驗した．茲で切り缺いた切口は翼弦に直角に切り下ろしたまゝで丸味を持たないものを扱つた．同じ寸法の切り缺きを有する翼と雖ども，それに用ひられた翼型が異なる時は翼の性能に及ぼす影響も異なるのではあるまいかと云ふ憶測の下に，異なる翼型に就いて同じ系統實驗を繰り返へした．一般に切り缺きのため翼の揚力係數曲線の迎角に對する傾きは減小し．又揚力零に對する迎角も減小する．但し對稱翼型の場合は揚力零に對する迎角は切り缺きに依つて變化しない．切り缺きの擴大により最大揚力係數及び最大揚抗比は減小し，最小抗力係數は増大する．壓力中心は切り缺きのため前方へ移動する．

---

(1) この研究の結果は旣に航空研究所彙報に發表されてゐる．實驗部分は彙報 No. 100, 102, 106, 108, 112, 116 及び 120 にある．理論的考察は No. 99, 105 及び 113 にあるがこの研究は今も尙續けられてゐる．

# No. 113.

(Published October, 1934.)

---

# The Experimental Investigation on the Effects of a Cut-out on the Wing Characteristics.[1]

By

Tetusi OKAMOTO, *Kôgakusi*,

Assistant of the Institute.

---

## Abstract.

The present paper is a summary of the experimental part of the results[2] investigated during last two years from autumn in 1932 until summer in 1934. The effects of extending the cut-out along span and extending it in the direction of chord were systematically tested for various wing sections, concerning with the aerofoil with rectangular cut-outs at the rear portion.

The value of $dc_z/d\alpha$ and the angle of incidence for no lift likewise decreases as the cut-out is extended. As an exception, however, an aerofoil of symmetrical section gives no effect on the angle for no lift due to cut-outs. The maximum values of both the lift coeffieient and the lift/drag ratio decrease, but conversely the minimum drag coefficient increases with extending the cut-out. The position of the centre of pressure moves forwards due to cut-out.

---

(1) Communicated by Prof. K. Wada.

(2) These results have already published in the Journal of the aeronautical research institute, Tokyo Imperial University. Experimental part are in No. 100, 102. 106, 108, 112, 116 and 120. Theoretical part are in No. 99, 105 and 113. And this investigation is further continued.

## 1. Introduction.

It is desirable for all aeroplanes to extend as much the range of sight as possible. To this purpose portions of the wing, usually at the centre, will be cut out although it produces large changes in the characteristics of the wing. The information of the effects of cut-outs on the characteristics of the wing is, thus, necessary and important for design of an aeroplane.

This problem has already investigated by Max Munk and G. Cario,(1) C. H. Powell,(2) J. Ackeret,(3) R. H. Smith,(4) H. Muttray,(5) I. Lotz(6) and recently A. Sherman.(7) But these results concern with the special cases or are unorganized to be of the greatest possible usefulness. The present experiments attempt to investigate systematically this problem to be useful for design.

## 2. Range of tests and description of models.

The present tests confined ourselves to the aerofoil with cut-outs of rectangular form in its rear portion, and moreover the rear edge of the cutaway section was not rounded, as is shown in Fig. 1.

---

(1) Max Munk und Günther Cario, Flügel mit Spalt in Fahrtrichtung. Technische Berichte I. (1917) p. 219.

(2) C. H. Powell, On the effects of cutting a hole in the top plane of a biplane. R. and M. No. 419 (1918).

(3) Ergebnisse der Aerodynamischen Versuchsanstalt zu Göttingen. Lieferung III. p. 83 and p. 92.

(4) R. H. Smith, Air force and moment for N-20 wing with certain cut-outs. N.A.C.A. Rept. No. 266 (1927).

(5) Ergebnisse der Aerodynamischen Versuchsanstalt zu Göttingen· Lieferung IV. p. 85

(6) I. Lotz, Theorie von Tragflügeln mit Auschnitten. Z.F.M. Nr. 14 (1933) p. 410.

(7) A. Sherman, The aerodynamic effects of wing cut-outs. N.A.C.A. Rept. No. 480 (1934).

The tests consist of two series:

a) Test of the effects of extending a cut-out along the span,

b) Test of the effects of extending a cut-out in the direction of the chord.

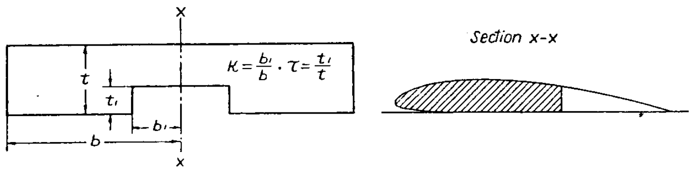


Fig. 1.

The models used in the test of (*a*) series are shown in Fig. 2. The width/span ratio (*k*) varies from 0·2 to 1·0 while the depth/chord ratio ($\tau$) retains 0·3.

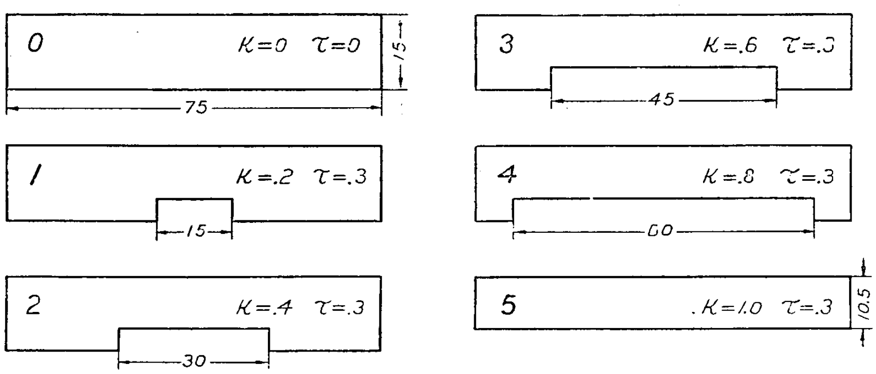


Fig. 2. Dimensions (in cm) of the models used in the test of the effects of extending a cut-out along the span.

The models used in the test of (*b*) series are shown in Fig. 3. The depth/chord ratio ($\tau$) varies from 0·1 to 1·0 while the width/span ratio (*k*) retains 0·2. In the case of a cut-out extending the full chord depth or the divided wing the parts cut away are connected with two cylindrical supports of diameter 8 mm and 6 mm.

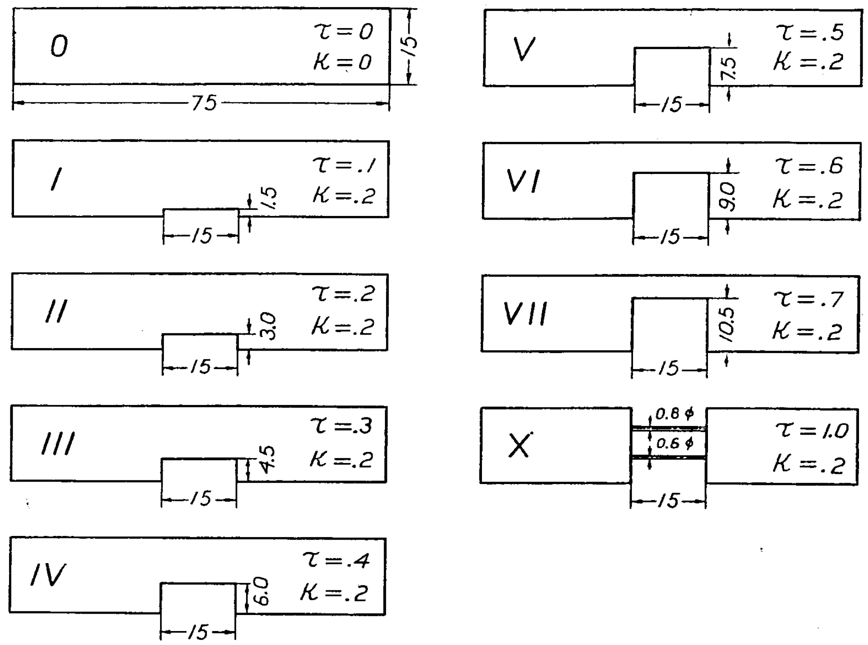


Fig. 3. Dimensions (in cm) of the models used in the test of the effects of extending a cut-out in the direction of the chord.

Under insight that the aerodynamic effects of a cut-out would be different according to the wing section although the cut-out has the same size, the above mentioned tests were repeated for three profiles Göttingen 593, Göttingen 459 and Sloane (mod).

Moreover, the *M*-12 wing was also tested but description of the results shall be omitted because the dimensions of cut-outs in this test are slightly different from the above test and the results give the similar effects of cut-out as those of the above mentioned profiles.

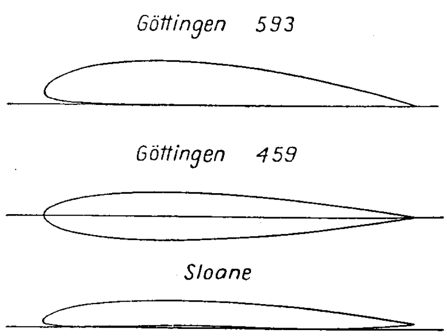


Fig. 4.

The tests were carried out in the small wind tunnel of diameter 1·5 metres of the institute at the wind velocity of about 30 m/sec. (Reynolds' number corresponds to about

$3 \cdot 10^5$), measuring the lift and drag for the angles of incidence between $-20°$ and $+26°$.

The chief dimensions of the original aerofoil are as follows:

Span = 75 cm, chord length = 15 cm, aspect ratio = 5,
and wing area = 1125 cm.$^2$

## 3. Calculation of coefficients.

(i) *Lift and drag coefficients.* The lift and drag coefficients are obtained by the equations

$$c_z = \frac{F_z}{qS} \quad \text{and} \quad c_x = \frac{F_x}{qS} - \Delta c_x ,$$

where $F_z$, $c_z$ lift force and lift coefficient,

$F_x$, $c_x$ drag (not corrected for the effect of the tunnel wall) and drag coefficient,

$S$ wing area of the original aerofoil,

$q$ dynamic pressure,

$\Delta c_x$ correction of drag coefficient for the effect of the tunnel wall.

Angles of incidence ($\alpha$) and values of drag have been corrected for the effect of the tunnel wall. That is

$$\Delta c_x = 0{\cdot}00796\, c_z^2 ,$$

$$\Delta \alpha = 0{\cdot}456\, c_z \quad \text{(degree)} .$$

(ii) *Moment coefficient and centre of pressure coefficient.* These coefficients are calculated by equations

$$c_m = \frac{M}{qSt} \quad \text{and} \quad c_p = \frac{s}{t} = \frac{-c_m}{c_z \cos \alpha + c_x \sin \alpha} ,$$

where $M$, $c_m$ moment about the leading edge and moment coefficient,

$c_p$ centre of pressure coefficient,

$t$ chord length of the original aerofoil,

$s$ distance of the centre of pressure behind the leading edge.

The moment will be regarded as positive in the sense that the angle of incidence tends to be increased.

Moreover, the coefficients of the aerofoil with out-cut extended full chord depth i.e. the divided aerofoil are calculated including the effects of two cylindrical supports.

## 4. Results of experiments.

### *A. Göttingen 593 wing.*

a) Effects of extending the cut-out along the span.

The results of the test are presented in figures from 5 to 9 where $c_z$, $c_x$, $c_m$, $c_p$ and $c_z/c_x$ curves are plotted against angle of incidence $\alpha$ and in figure 10 where $c_z$ is plotted against $c_x$.

(i) *Lift coefficient.* The variation of lift coefficient due to cut-out is noticeable, as is shown in Fig. 5. The slope of the lift curve and the angle for zero lift likewise decreases as the width of cut-out increases. The maximum lift coefficient decreases, but the value based on the actual wing area increases with the width, as is shown in Fig. 11. The stalling angle tends to increase as the width increases.

(ii) *Drag coefficient.* The curves of the drag coefficient, as is shown in Fig. 6, intersect each other at $\alpha = \pm 5{\cdot}8^{\circ}$ where the drag coefficien is independent to the width of cut-out. At smaller angles of incidence than this angle the drag coefficient increases with the width and conversely it decreases at larger angles.

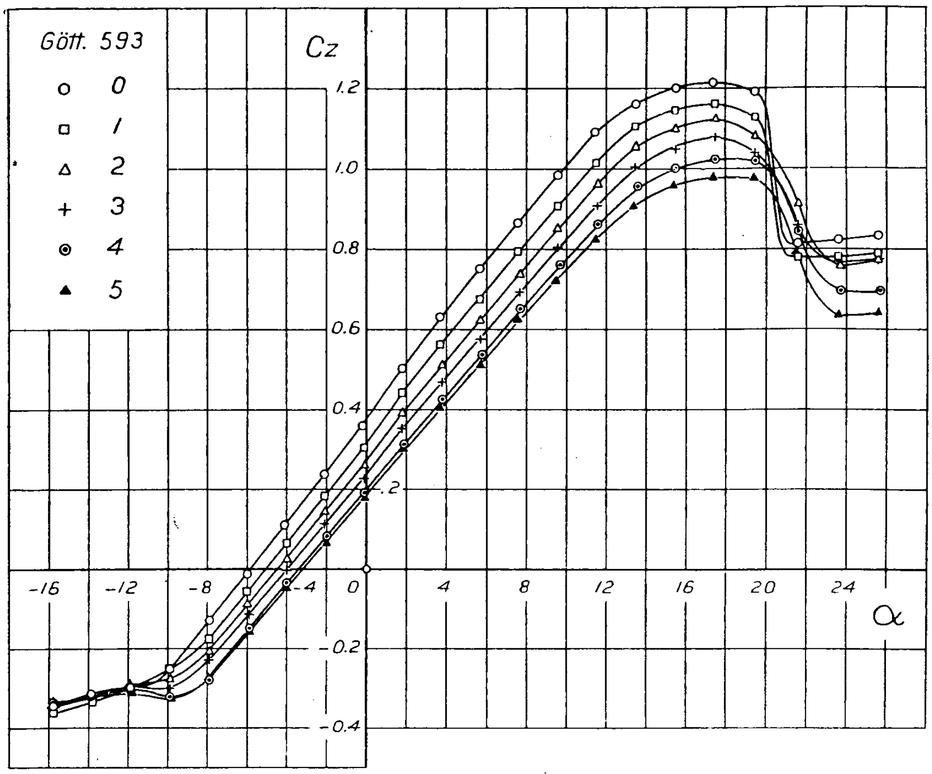


Fig. 5. Curves of the lift coefficient.

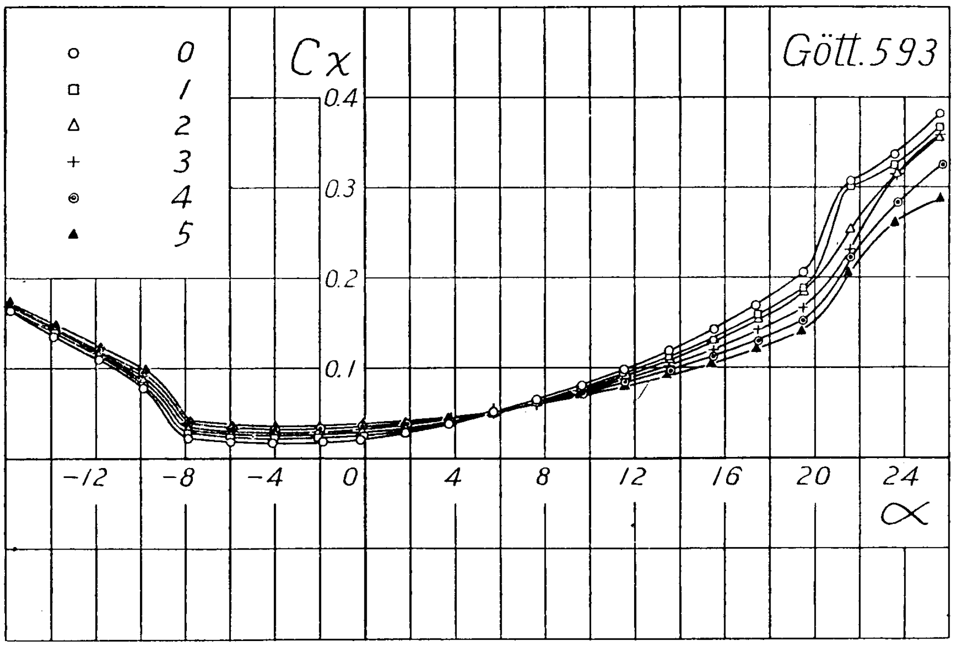


Fig 6. Curves of the drag coefficient.

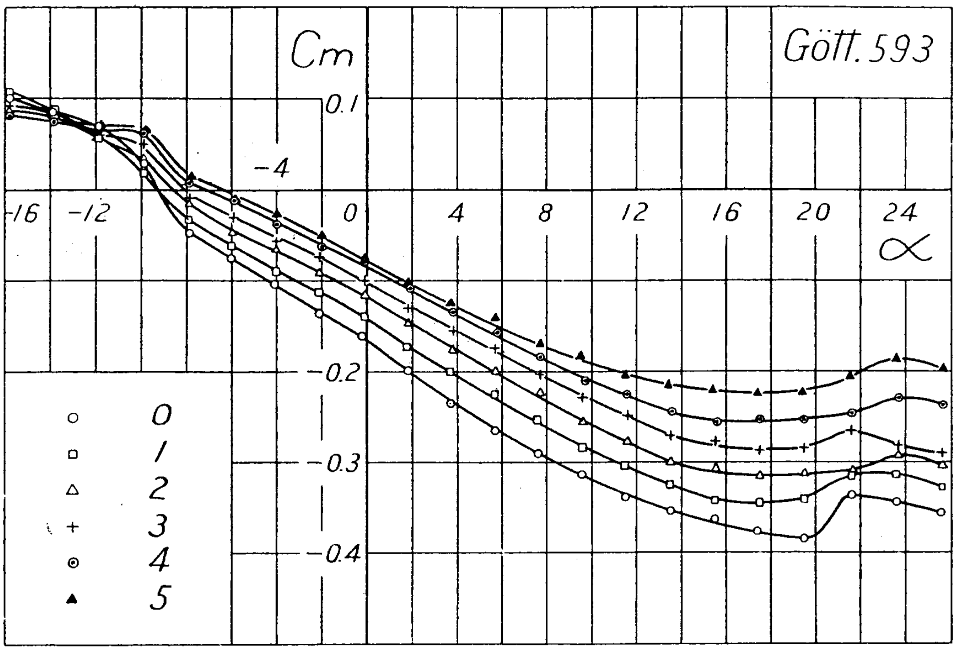


Fig. 7. Curves of the moment coefficient.

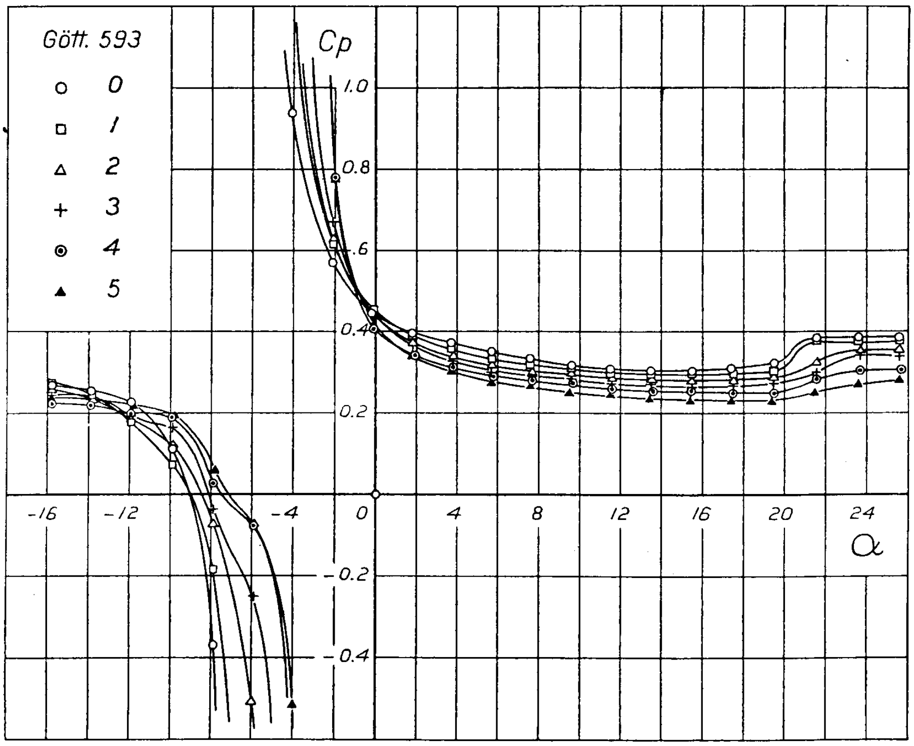


Fig. 8. Curves of the centre of pressure coefficient.

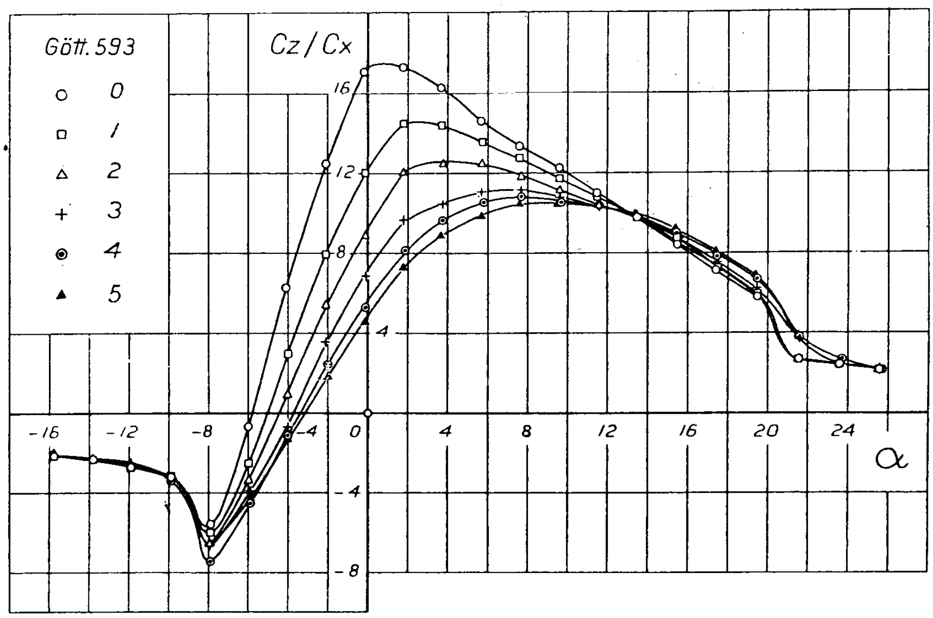


Fig. 9. Curves of the lift/drag ratio.

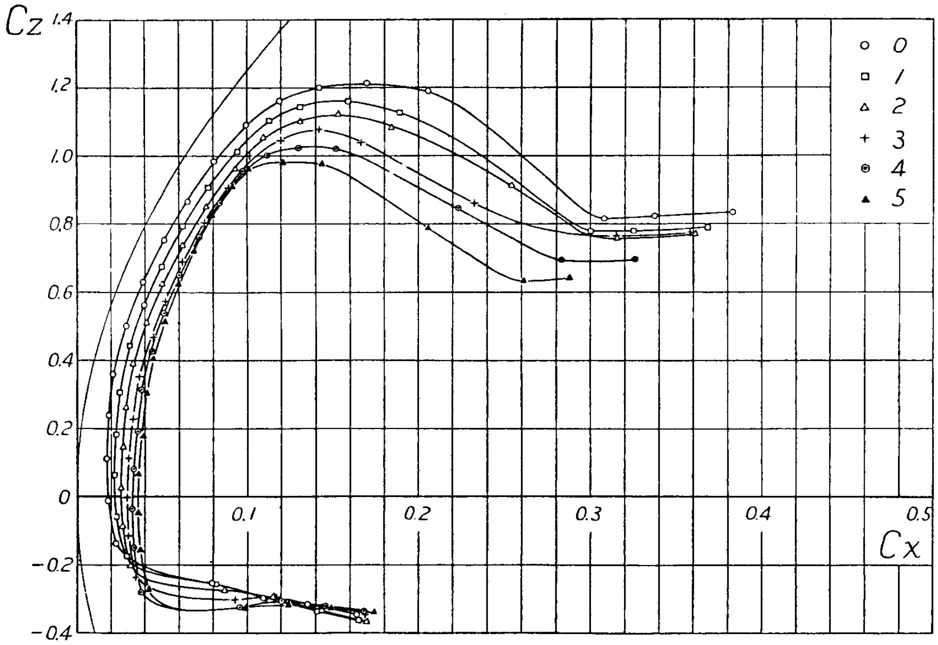


Fig. 10. Polar curves.

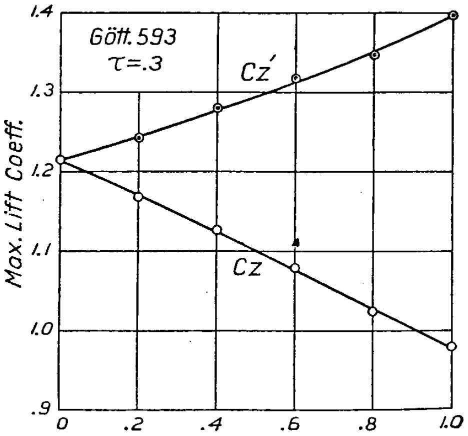


Fig. 11. Variation of the maximum lift coefficient due to the width of cut-out. Cz' denotes the value based on the actual wing area.

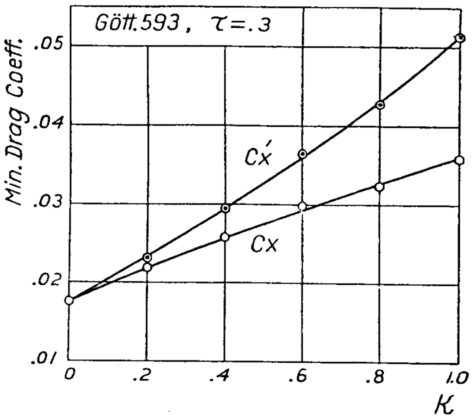


Fig. 12. Variation of the minimum drag coefficient due to the width of cut-out. Cx' denotes the value based on the actual wing area.

The polar curves shown in Fig. 10 indicate that the profile drag coefficient increases exceedingly with the width while the effect on the induced drag is almost negligible.

(iii) *Moment coefficient and centre of pressure coefficient.* The moment coefficient decreases as the width of cut-out increases, as is shown in Fig. 7. The curves of the centre of pressure coefficient which are shown in Fig. 8 intersect each other at $\alpha \doteqdot -1°$. At larger angles than this angle the position of the centre of pressure moves forwards in a nearly linear relation with the width of cut-out.

(iv) *Lift drag ratio.* The curves of lift/drag ratio are presented in Fig. 9. The maximum value of lift/drag ratio decreases as the width of cut-out increases.

### b) Effects of extending the cut-out in the direction of the chord.

(i) *Lift coefficient.* Fig. 13 shows the variation of the lift coefficient due to the depth of cut-out. The slope of the lift curve and the

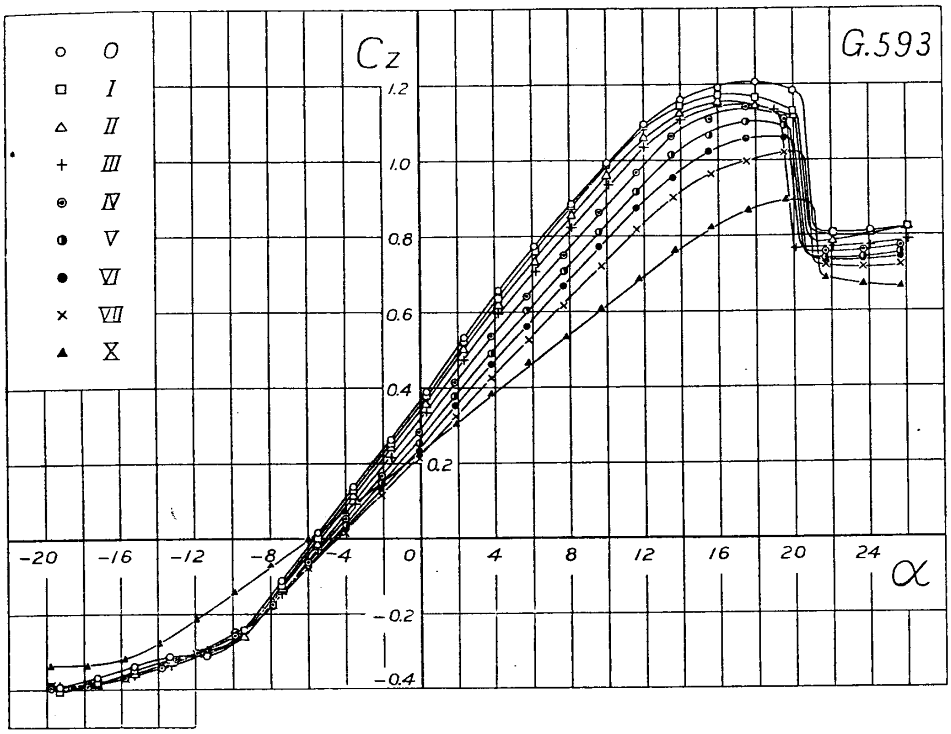


Fig. 13. Curves of the lift coefficient.

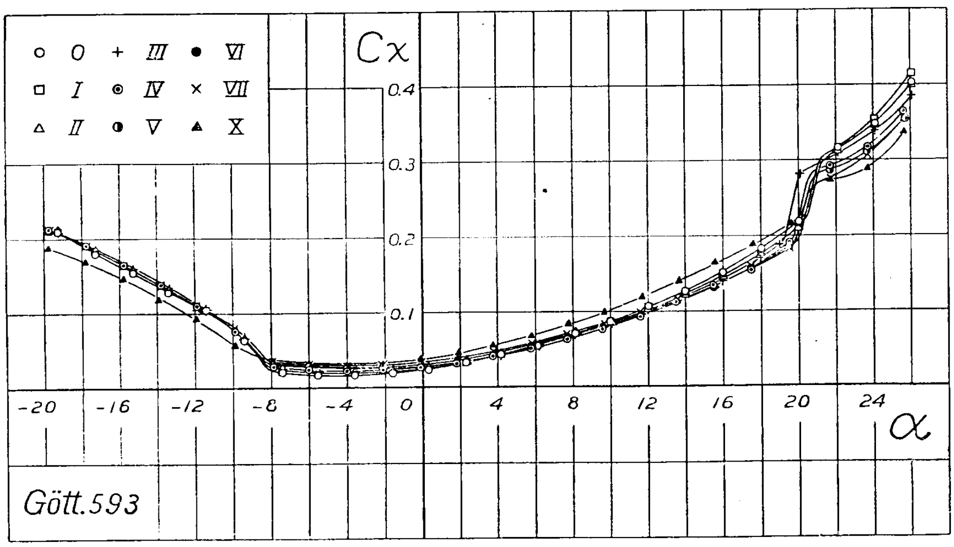


Fig. 14. Curves of the drag coefficient.

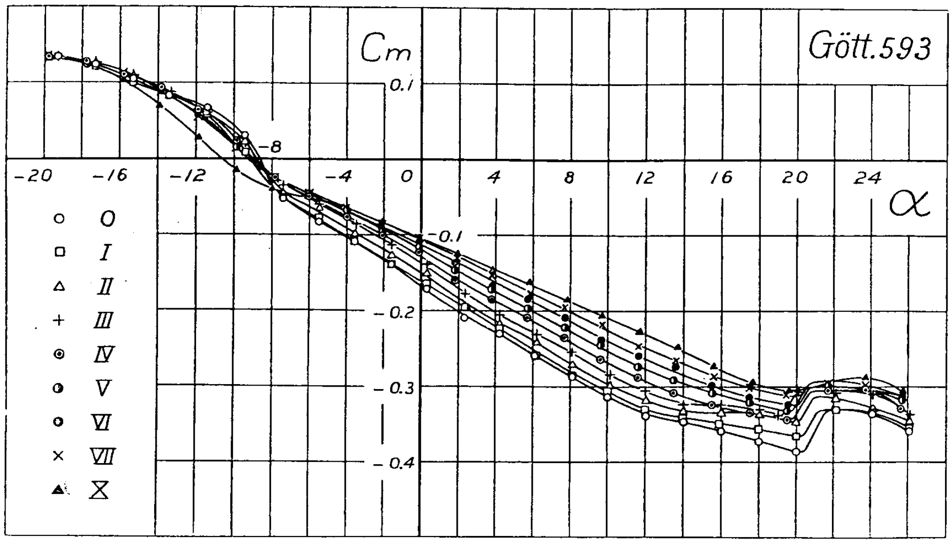


Fig. 15. Curves of the moment coefficient.

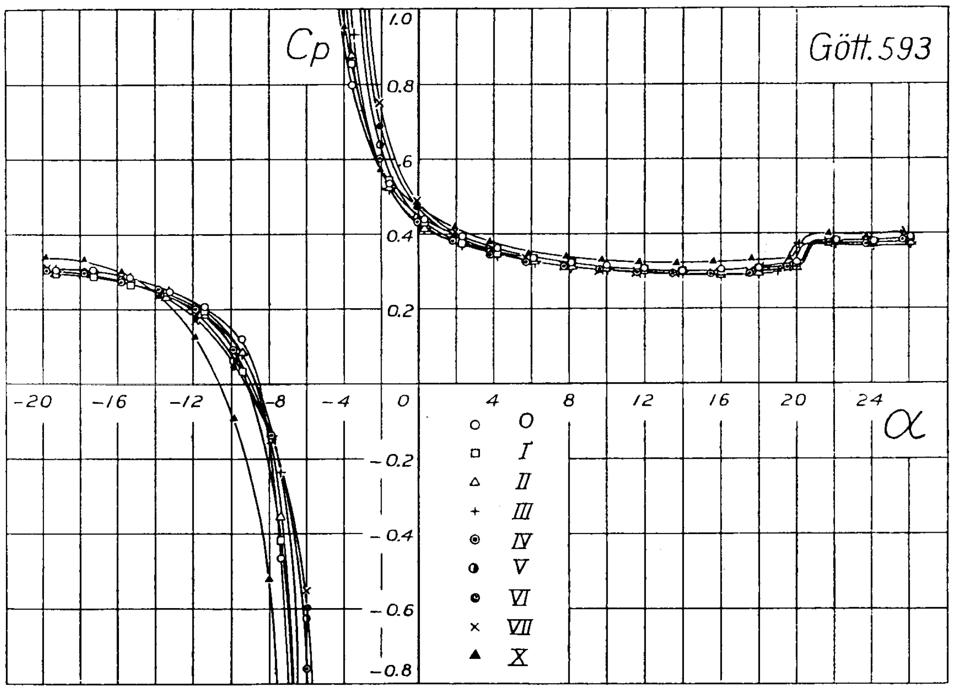


Fig. 16. Curves of the centre of pressure coefficient.

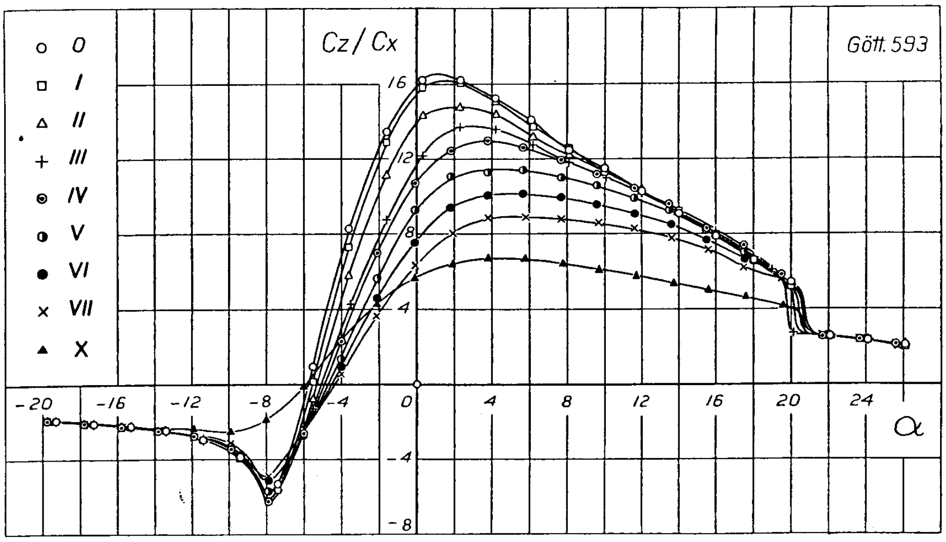


Fig. 17. Curves of the lift/drag ratio.

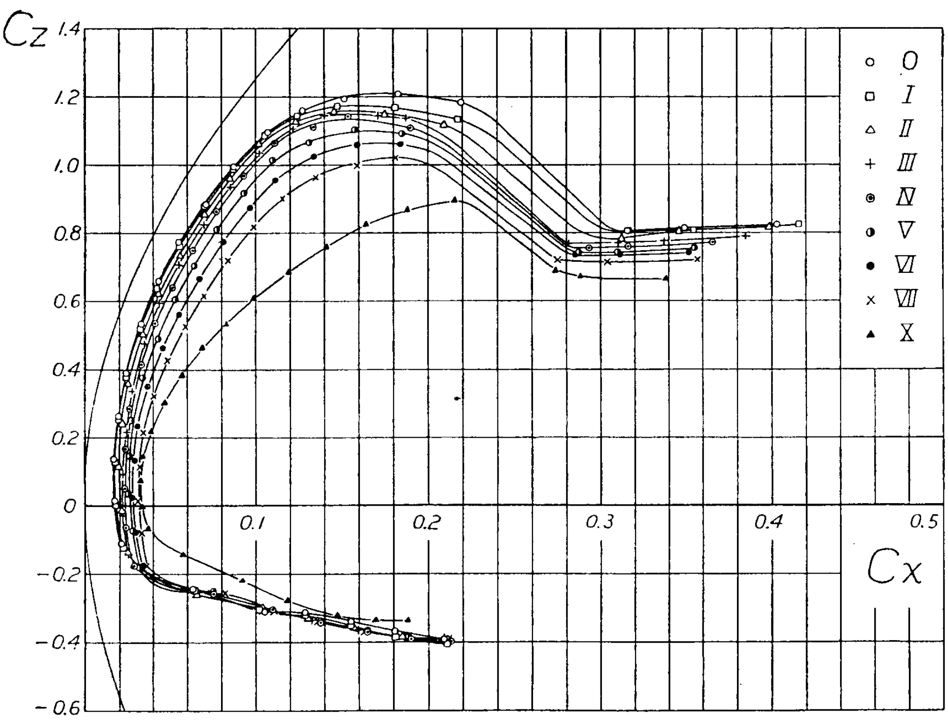


Fig. 18. Polar curves.

angle for zero lift likewise decreases as the depth of cut-out increases. In the case of the divided aerofoil, however, the zero lift angle is not different from that of the original aerofoil. The maximum lift coefficient decreases as the depth increases, as is shown in Fig. 19.

Comparing the results of this test with those of the preceding test, the lift coefficient of the aerofoil with cut-out for small angles of incidence can be written, for $\tau<0{\cdot}5$ and all values of $k$, by the equation

$$c_z = \bar{c}_z \cdot L - \bar{c}_{z0} \,.\, N\,,$$

where $$L = 1 - 1{\cdot}217\,\tau^2 k\,(2-k)$$

and $$N = 1{\cdot}103\,\tau k\,(2-k)\,,$$

being $\bar{c}_z$ and $\bar{c}_{z0}$ the lift coefficient and that at zero angle of incidence of the original aerofoil respectively.

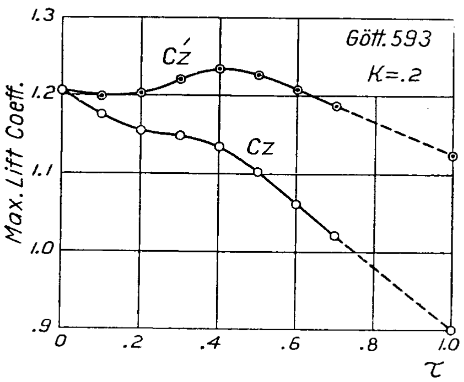


Fig. 19. Variation of the maximum lift coefficient due to the depth of cut-out. Cz′ denotes the value based on the actual wing area.

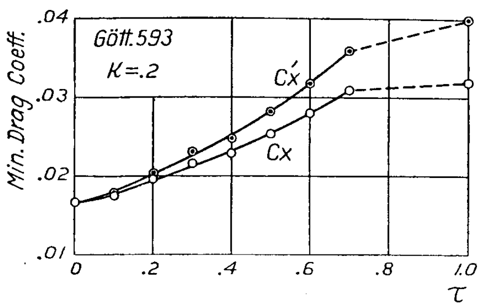


Fig. 20. Variation of the minimum drag coefficient due to the depth of cut-out. Cx′ denotes the value based on the actuat wing area.

(ii) *Drag coefficient.* Fig. 14 shows the variation of the drag coefficient due to the depth of cut-out. The polar curves shown in Fig. 18 indicate that the profile drag increases exceedingly with the depth and the induced drag tends to increase only when the depth of cut-out becomes considerably large. The minimum drag coefficient increases with the depth, as is shown in Fig. 20.

(iii) *Moment coefficient and centre of pressure coefficient.* The moment coefficient decreases as the depth of cut-out increases, as is shown in Fig. 15. Fig. 16 shows that the variation of the centre of pressure coefficient due to the depth is not so much severe as due to the width.

(iv) *Lift drag ratio.* The maximum value of lift/drag ratio decreases as the depth of cut-out increases, as is shown in Fig. 17. Moreover, the values of the lift/drag ratio at the angles after stall are seen to be independent to the cut-out.

### *B. Göttingen 459 wing.*

a) Effects of extending the cut-out along the span.

(i) *Lift coefficient.* The curves of the lift coefficient are shown in Fig. 21. The slope of the lift curve decreases as the width of cut-out

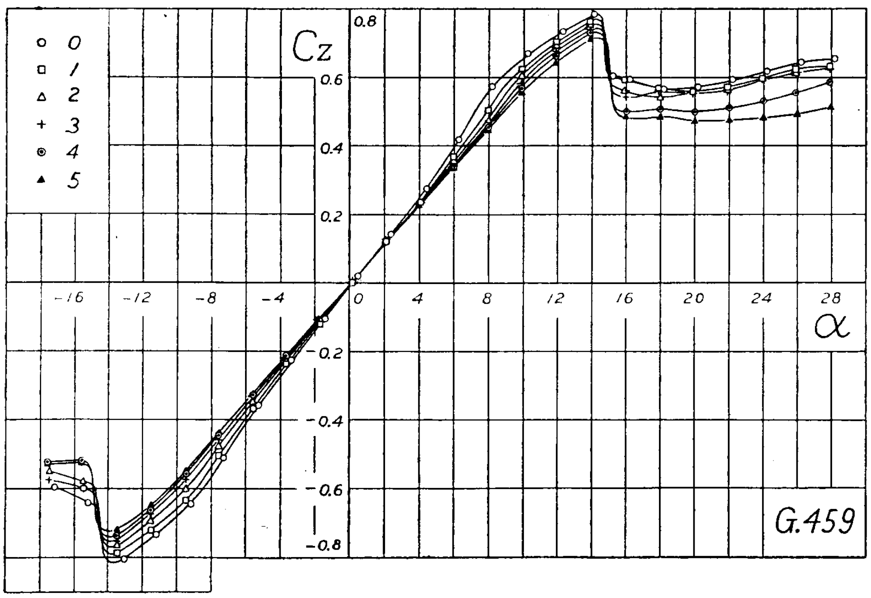


Fig. 21. Curves of the lift coefficient.

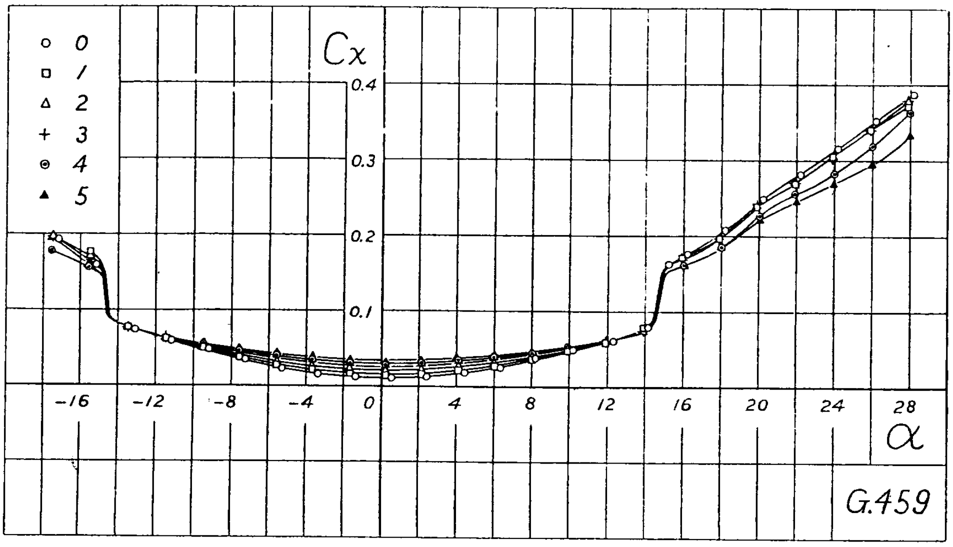


Fig. 22. Curves of the drag coeffieient.

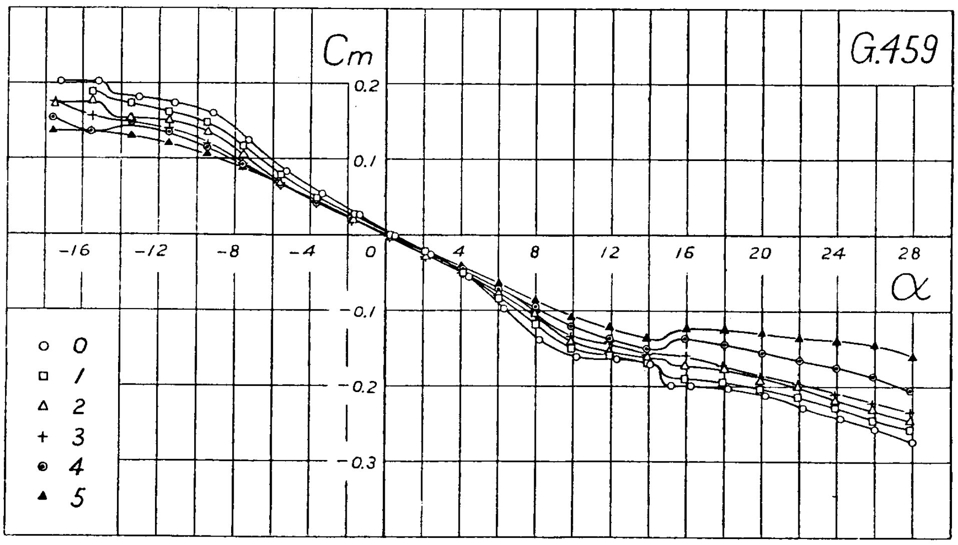


Fig. 23. Curves of the moment coefficient.

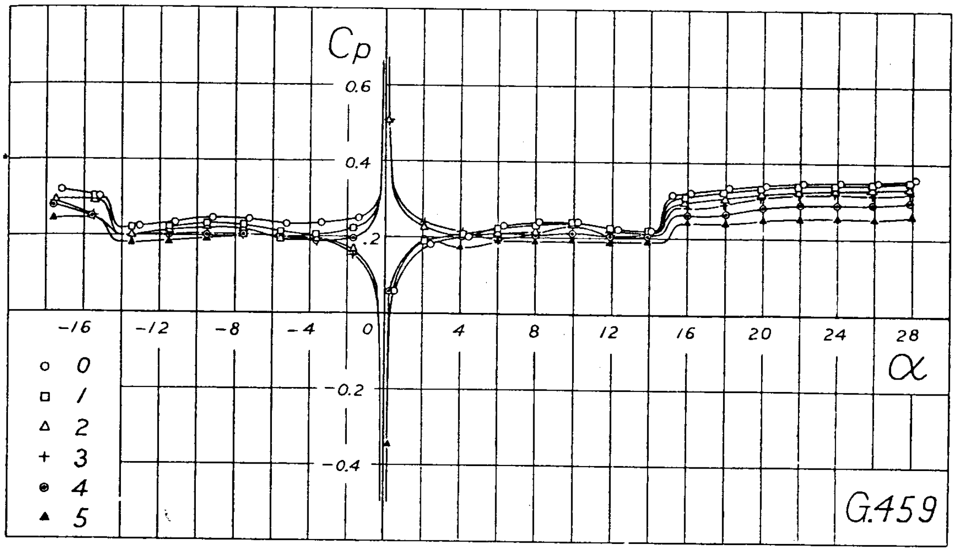


Fig. 24. Curves of the centre of pressure coefficient.

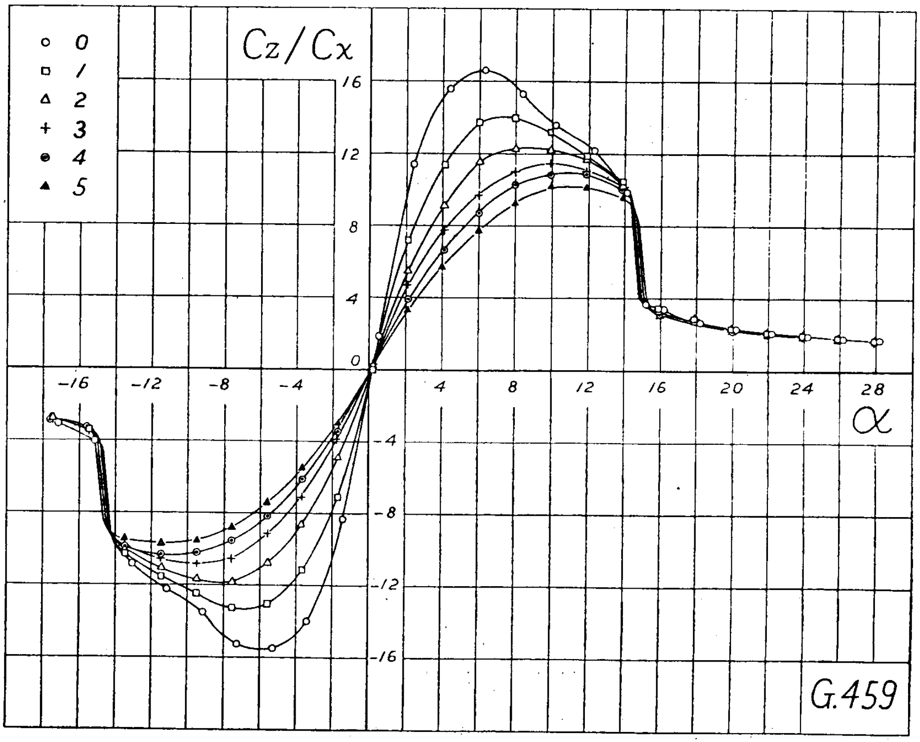


Fig. 25. Curves of the lift/drag ratio.

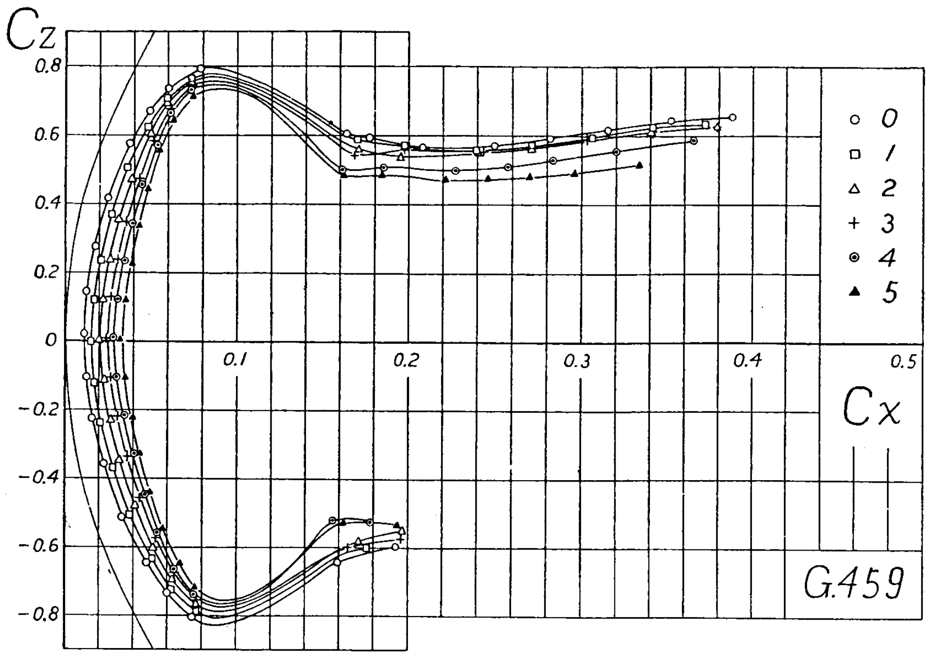


Fig. 26. Polar curves.

increases in the same manner as the preceding test. In this case, however, the angle of incidence for zero lift is not affected by the cut-out. The empirical formula obtained in the preceding article is also applicable in this case provided $\bar{c}_{z0}$ is put to be zero.

The maximum lift coefficient decreases as the width of cut-out increases, as is shown in Fig. 27.

The comparison of the results of the Göttingen 459 wing with those of the Göttingen 593 wing shows that a wing with the symmetrical section gives a smaller decrease of the lift coefficient due to cut-out than a wing with the cambered profile.

(ii) *Drag coefficient.* Fig. 22 shows the variation of the drag coefficient due to the width of cut-out. The curves intersect each other at $\alpha \doteqdot 12^\circ$ where the drag coefficient is independent to the width of cut-out. At larger angles of incidence than this value the drag coefficient decreases, but at smaller angles it increases with the width. The minimum drag coefficient increases, thus, as the width of cut-out increases, as is shown in Fig. 28.

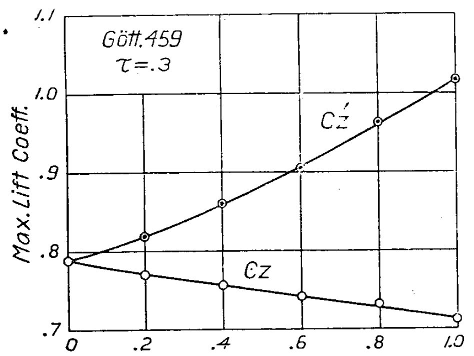


Fig. 27. Variation of the maximum lift coefficient due to the width of cut-out. Cz′ denotes the value based on the actual wing area.

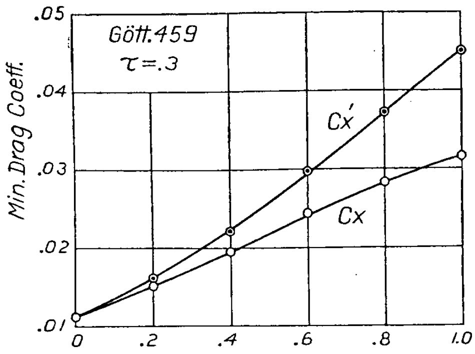


Fig. 28. Variation of the minimum drag coefficient due to the width of cut-out. Cx′ denotes the value based on the actual wing area.

(iii) *Moment coefficient and centre of pressure coefficient.* The moment coefficient and the centre of pressure coefficient, which are shown in Figs. 23 and 24 respectively, decreases as the width of cut-out increases. Namely, the position of the centre of pressure moves forwards with extending the cut-out along span.

(iv) *Lift/drag ratio.* The lift/drag ratio decreases as the width of cut-out increases, as is shown in Fig. 25. But at angles of incidence after stall the ratio is seen to be independent to the width of cut-out.

## b) Effects of extending the cut-out in the direction of the chord.

(i) *Lift coeffieient.* The curves of the lift coefficient are shown in Fig. 29. The slope of the lift curve against angle of incidence decreases, but the zero lift angle is not affected with the depth of cut-out. The maximum lift coefficient decreases, as is shown in Fig. 35, and the stalling angle tends to increase as the depth of cut-out increases.

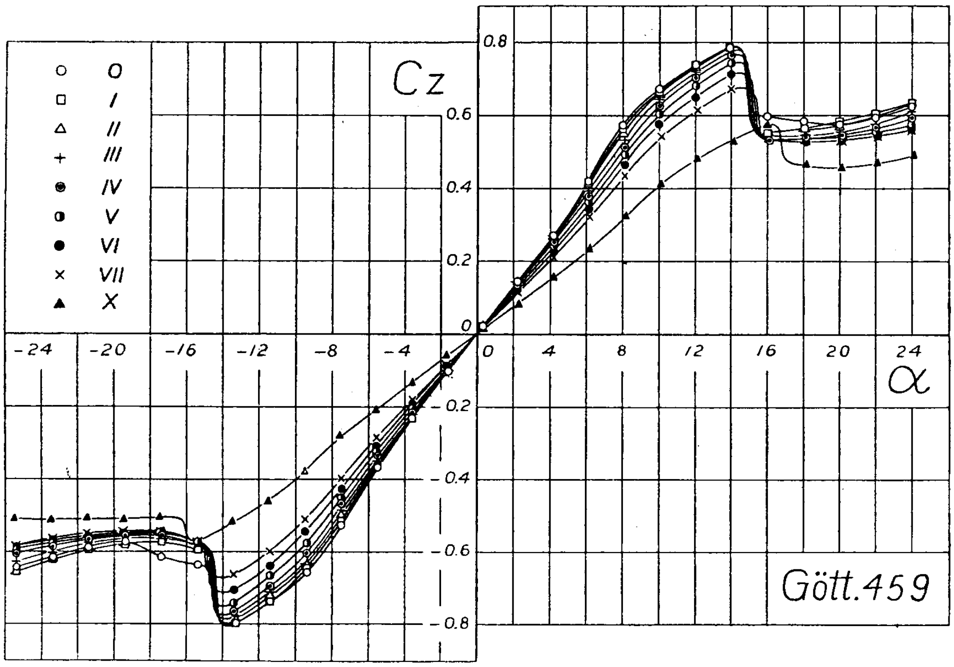


Fig. 29. Curves of the lift coefficient.

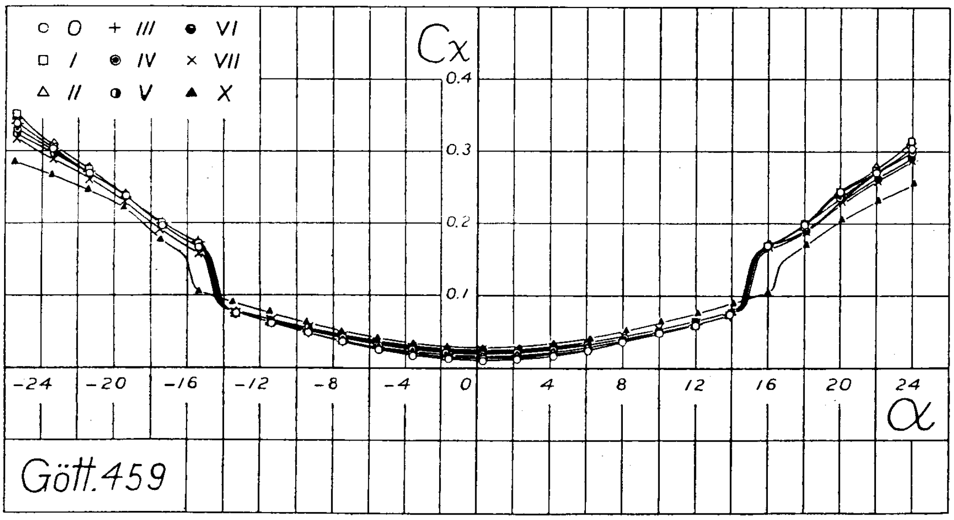


Fig. 30. Curves of the drag coefficient.

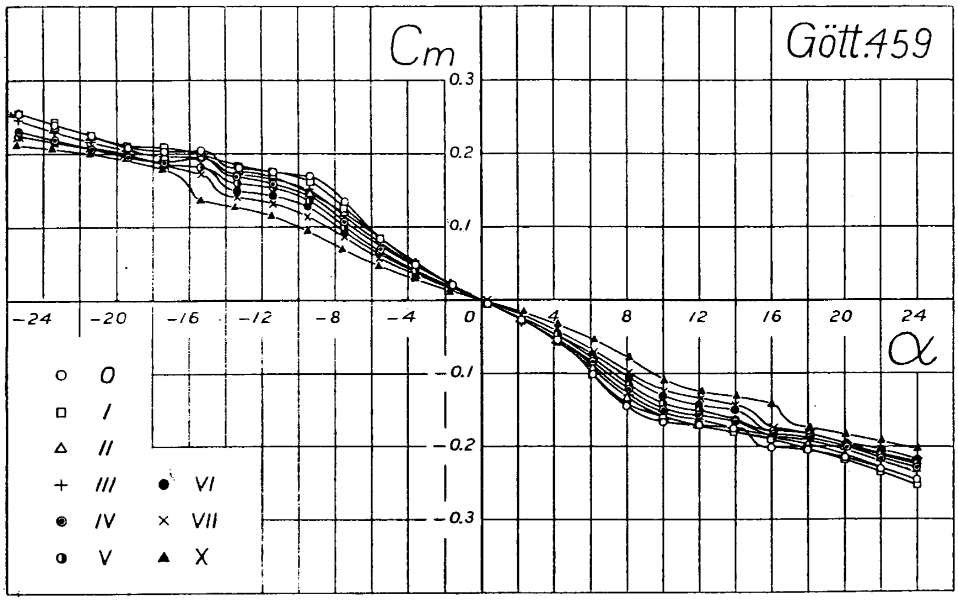


Fig. 31. Curves of the moment coefficient.

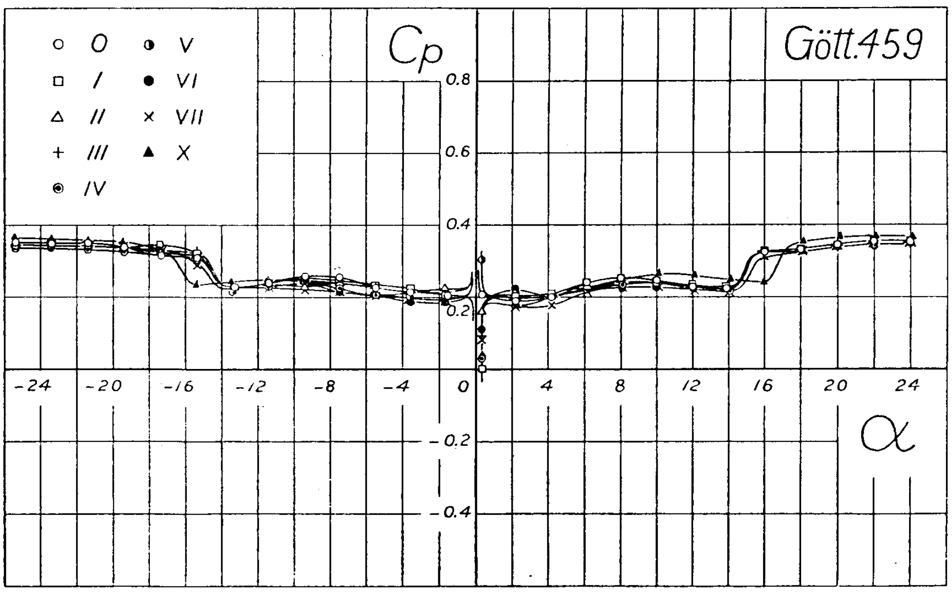


Fig. 32. Curves of the centre of pressure coefficient.

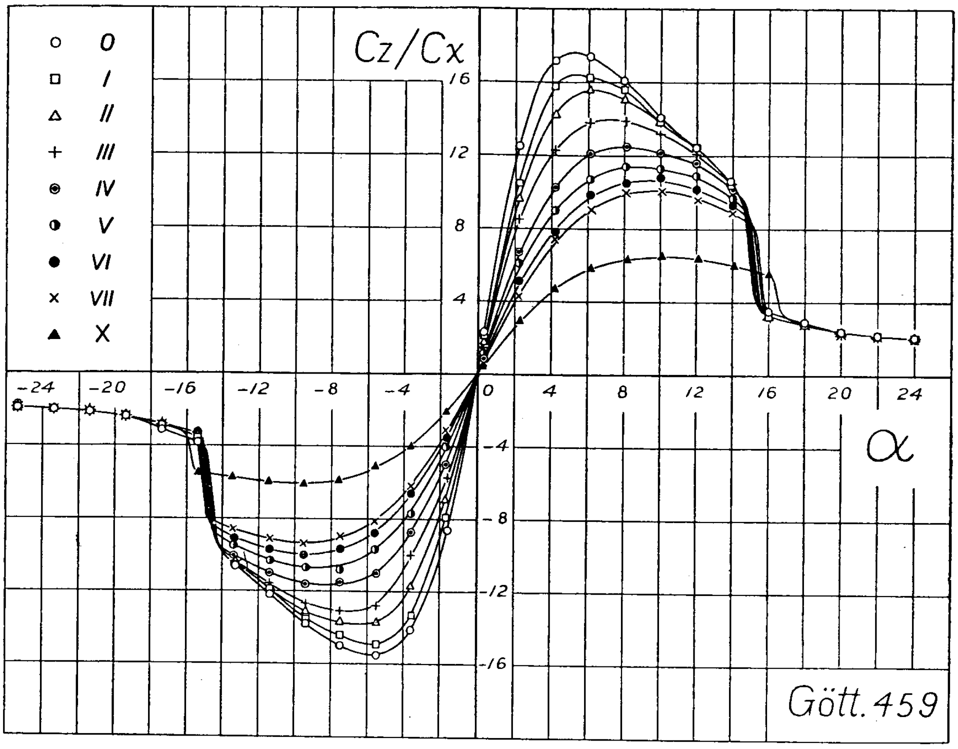


Fig. 33. Curves of the lift/drag ratio.

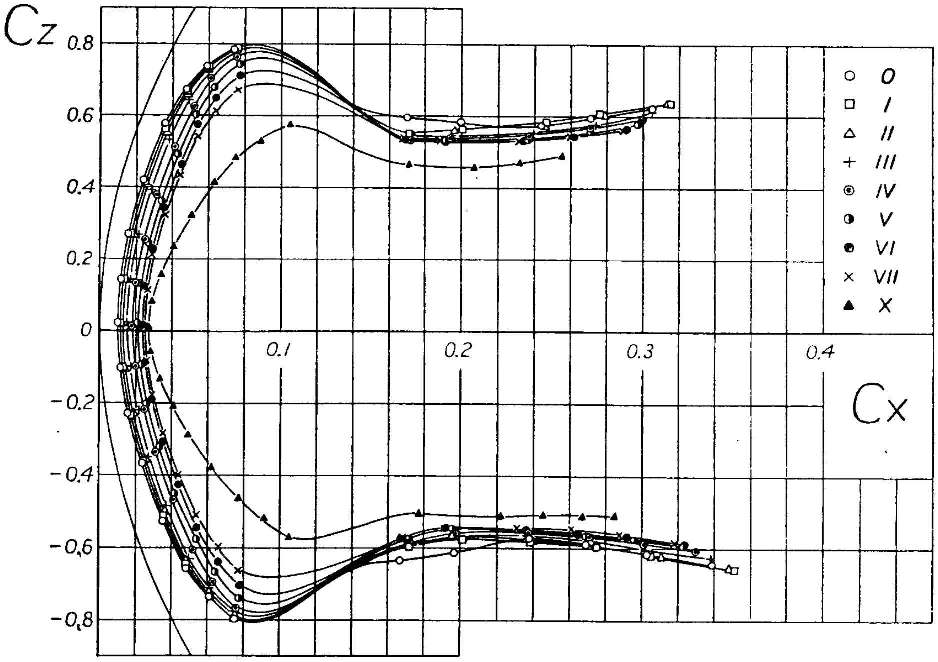


Fig. 34. Polar curves.

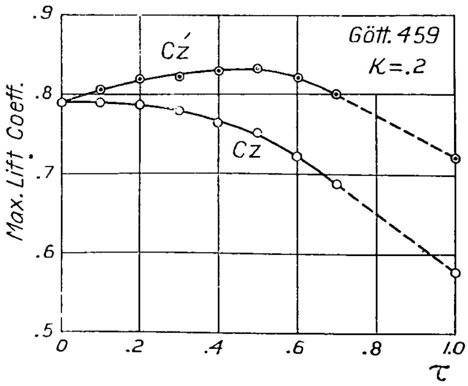


Fig. 35. Variation of the maximum lift coefficient due to the depth of cut-out. Cz′ denotes the value based on the actual wing area.

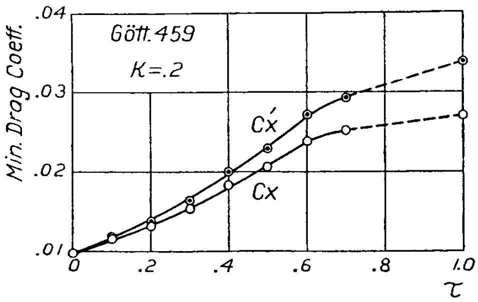


Fig. 36. Variation of the minimum drag coefficient due to the depth of cut-out. Cx′ denotes the value based on the actual wing area.

(ii) *Drag coefficient.* Fig. 30 shows the variation of the drag coefficient due to the depth of cut-out. The minimum drag coefficient increases with the depth, as is shown in Fig. 36. The profile drag increases exceedingly, but the induced drag is not almost affected with the depth. However, in the case of the divided aerofoil the induced drag increases considerably.

(iii) *Moment coefficient and centre of pressure coefficient.* The moment coefficient decreases as the depth increases, as is shown in Fig. 31. The centre of pressure coefficient is not almost affected with the depth.

(iv) *Lift/drag ratio.* The lift/drag ratio decreases as the depth increases, as is shown in Fig. 33. After stall it is seen to be independent to the cut-out.

## C. *Sloane wing.*

### a) Effects of extending the cut-out along the span.

(i) *Lift coefficient.* The slope of the lift curve decreases at the larger rate than that of the wings Göttingen 593 and 459. The zero lift

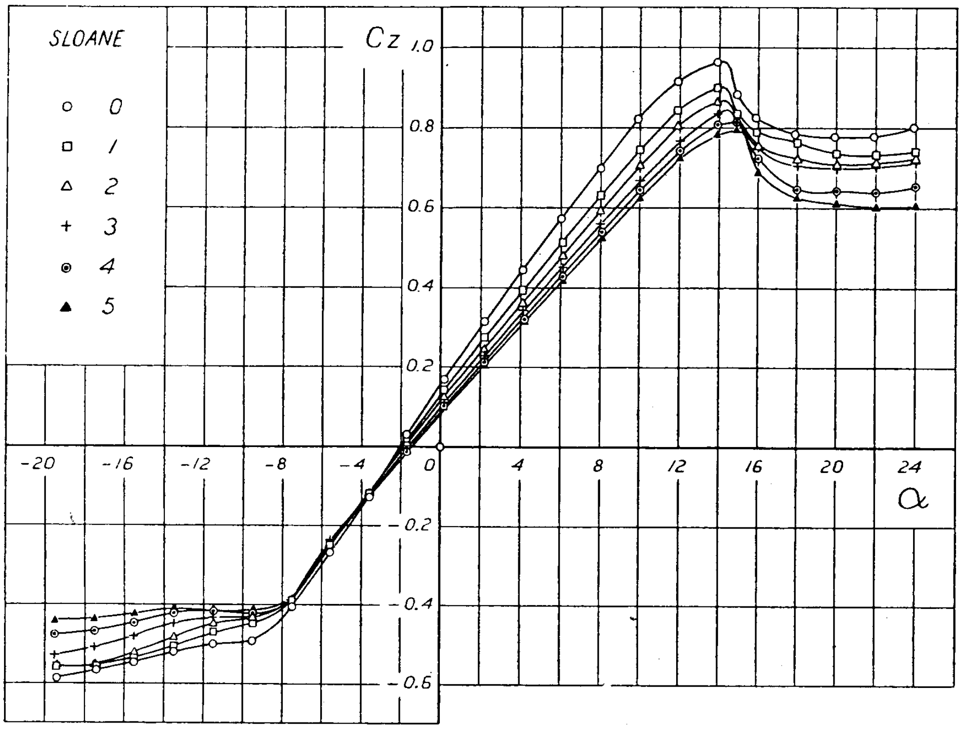


Fig. 37. Curves of the lift coefficient.

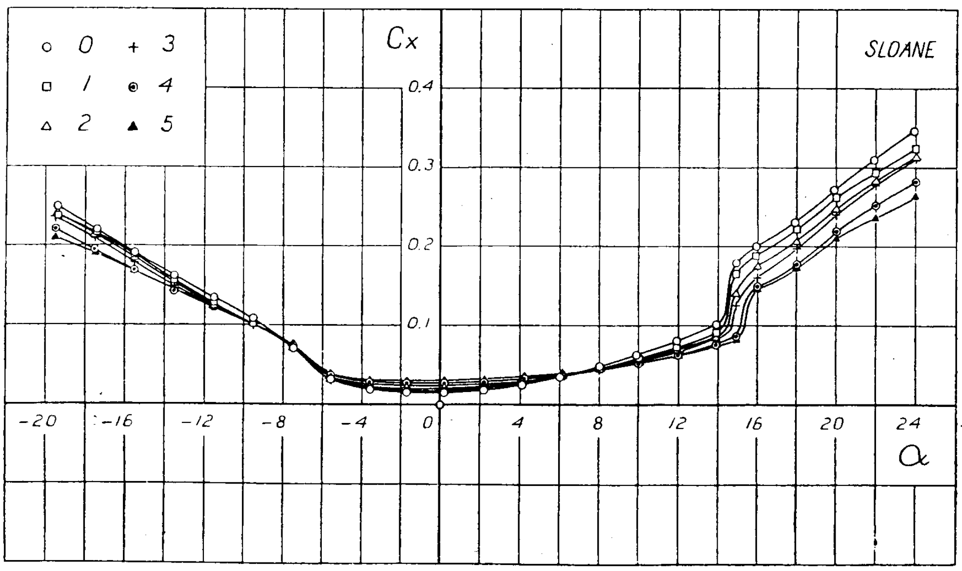


Fig. 38. Curves of the drag coefficients.

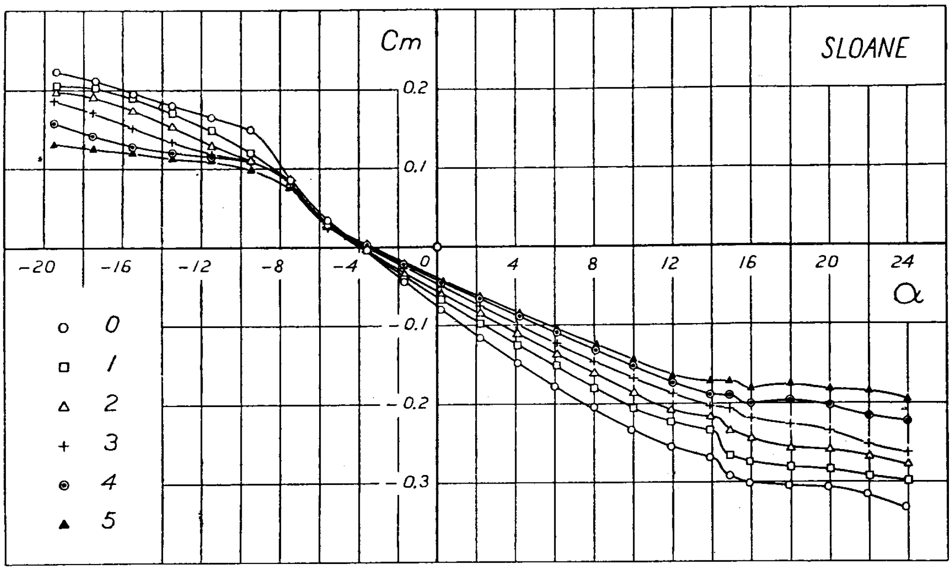


Fig. 39. Curves of the moment coefficient.

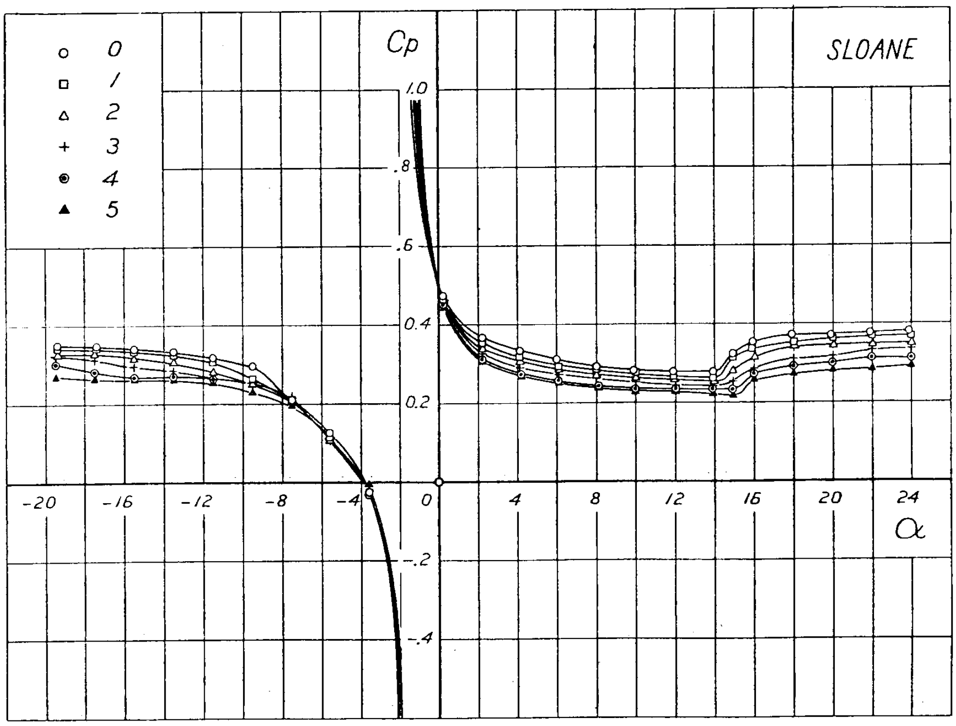


Fig. 40. Curves of the centre of pressure coefficient.

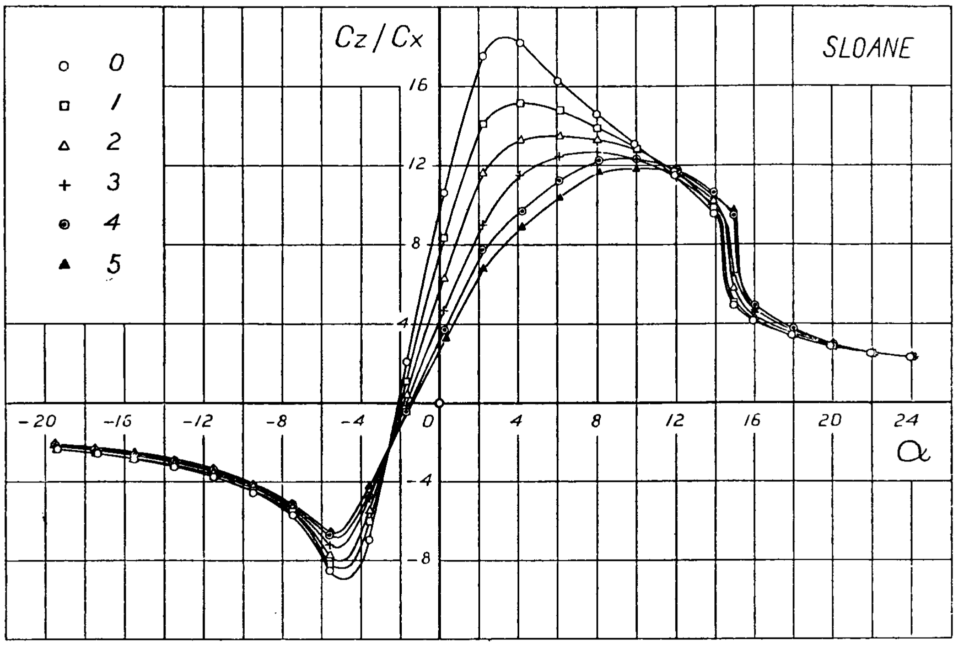


Fig. 41. Curves of the lift/drag ratio.

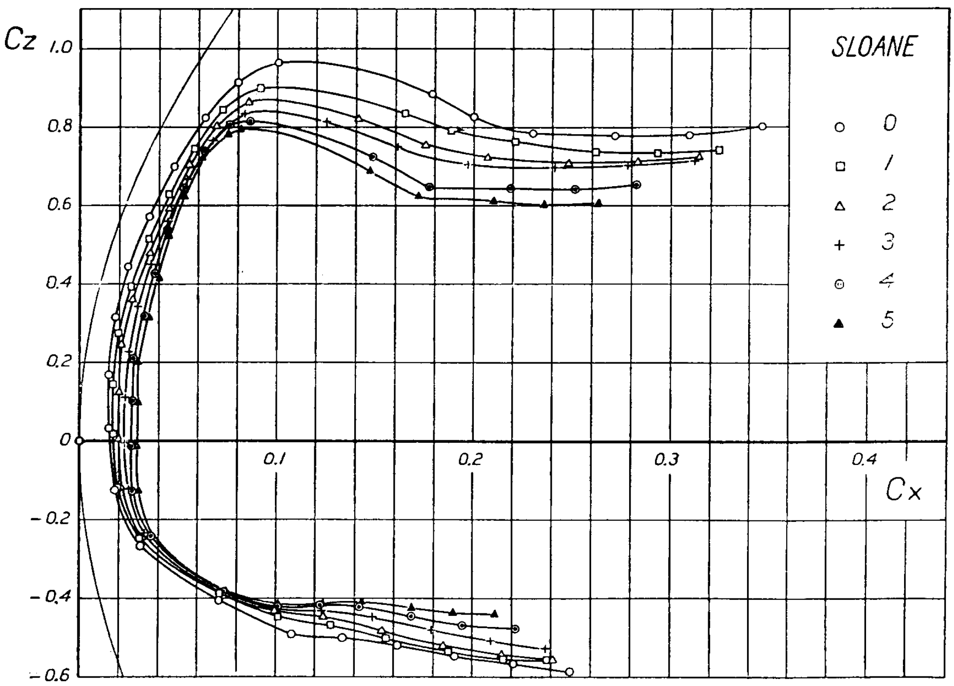


Fig. 42. Polar curves.

angle decreases slightly as the width increases. The maximum lift coefficient decreases, as is shown in Fig. 43, and the stalling angle tends to increase with the width.

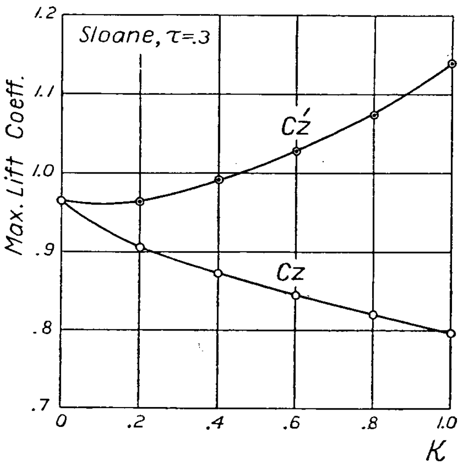


Fig. 43. Variation of the maximum lift coefficient due to the width of cut-out. Cz′ denotes the value based on the actual wing area.

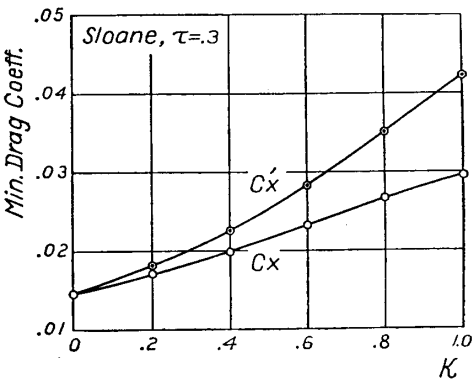


Fig. 44. Variation of the minimum drag coefficient due to the width of cut-out. Cx′ denotes the value based on the actual wing area.

(ii) *Drag coeffieient.* The curves of the drag coefficient, which are shown in Fig. 38, intersect each other at two points $\alpha = +7^\circ$ and $-8^\circ$ where the drag coefficient is independent to the width of cut-out. At the angles of incidence between $-8^\circ$ and $+7^\circ$ the drag coefficient increases and at angles outside of this range it decreases as the width of cut-out increases. The minimum drag coefficient increases with the width, as is shown in Fig. 44.

(iii) *Moment coefficient and csntre of preesure coefficient.* The moment coefficient decreases as the width increases, as is shown in Fig. 39. The curves of the centre of pressure coefficient, which are shown in Fig. 40, intersect each other at $\alpha \doteqdot 0^\circ$ and at larger angles than this value the position of the centre of pressure moves forwards as the width of cut-out increases.

(iii) *Lift/drag ratio.* Fig. 41 shows the variation of the lift/drag ratio due to the width of cut-out. The maximum value of the lift/drag ratio decreases as the width increases. But the lift/drag ratio at the angles after stall is seen to be independent to the width of cut-out.

## b) Effects of extending the cut-out in the direction of the chord.

(i) *Lift coefficient.* The curves of the lift coefficient are shown in Fig. 45. The slope of the lift curve against angle of incidence and the angle for zero lift likewise decreases as the depth of cut-out increases. In the case of a cut-out extending the full chord depth i.e. the divided wing, however, the zero lift angle is not different from that of the original aerofoil. The lift curves of the aerofoils from 0 to VII intersect each other at $\alpha = -4{\cdot}5^{\circ}$ where the lift coefficient is independent to the depth of cut-out. The maximum lift coefficicnt decreases, as is shown in Fig. 51, but the stalling angle tends to increase with the depth.

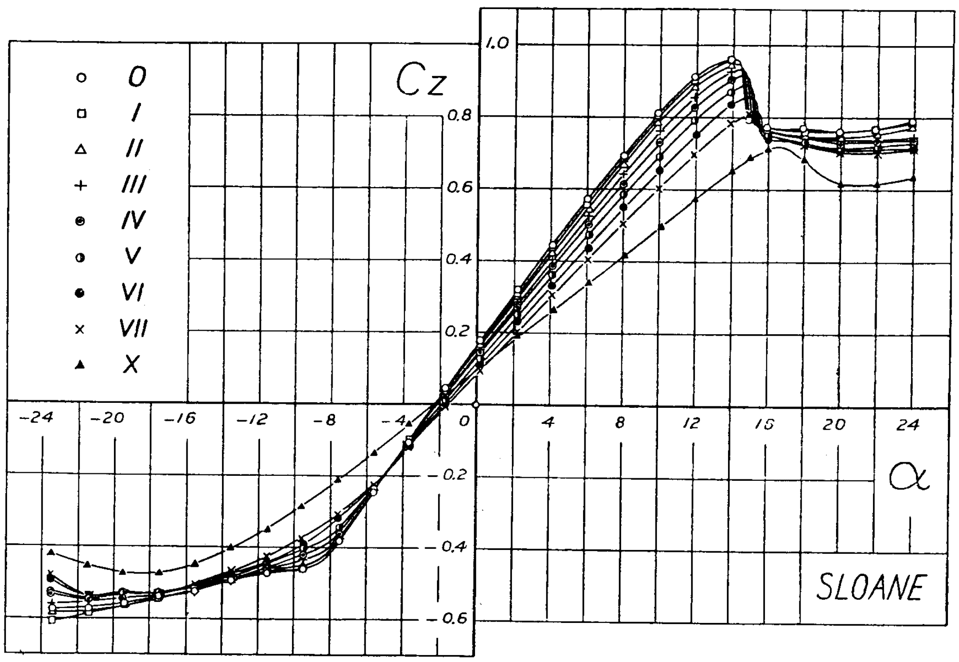


Fig. 45. Curves of the lift coefficient.

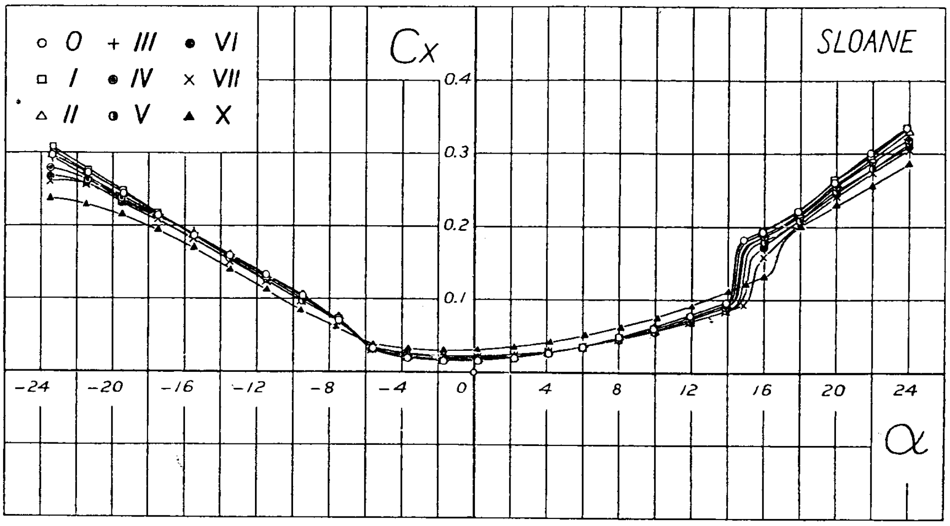


Fig. 46. Curves of the drag coefficient.

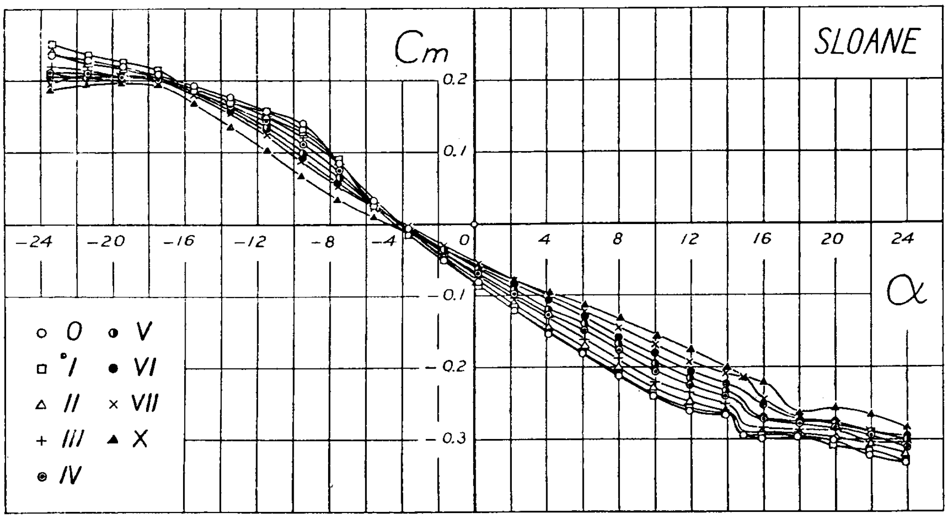


Fig. 47. Curves of the moment coefficient.

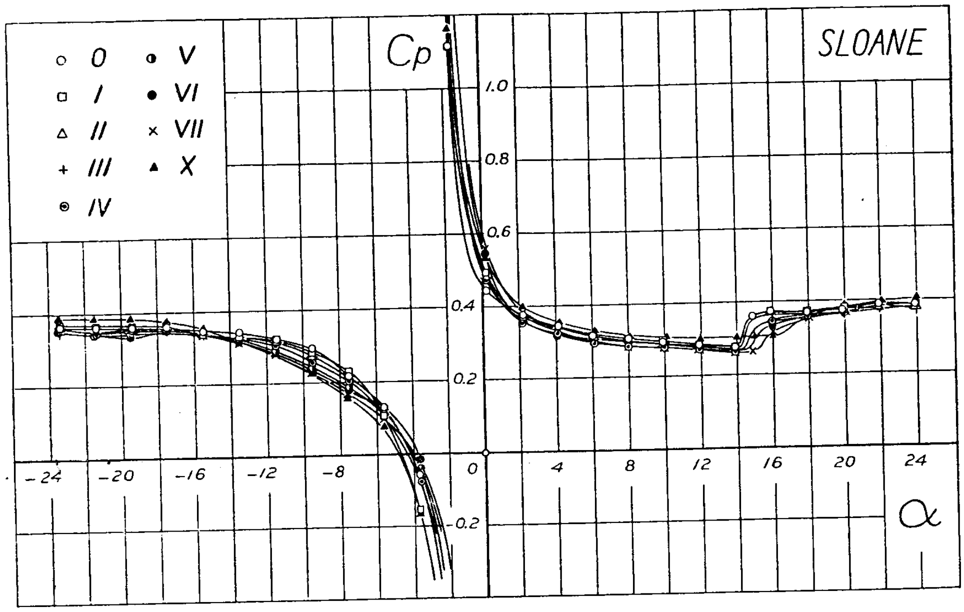


Fig. 48. Curves of the centre of pressure coefficient.

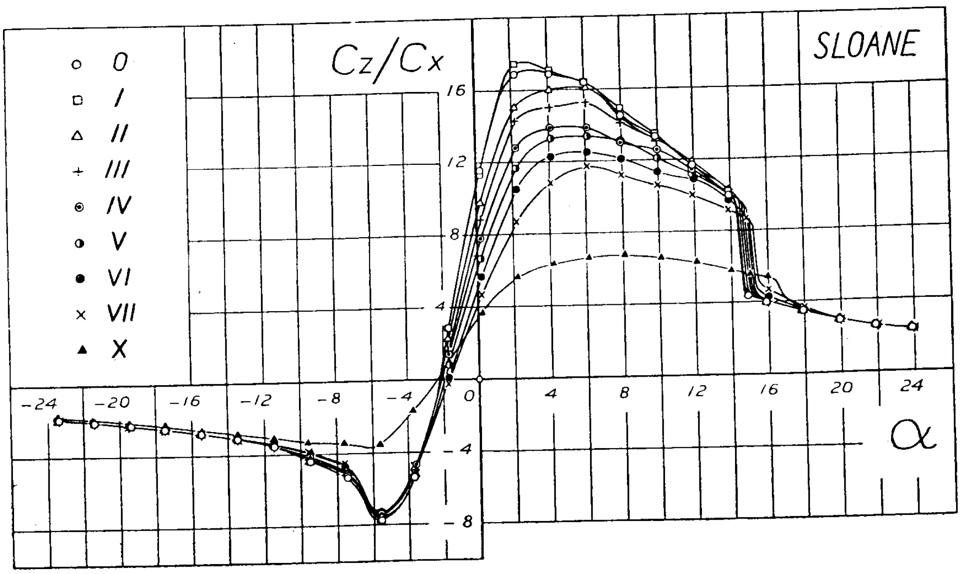


Fig. 49. Curves of the lift/drag ratio.

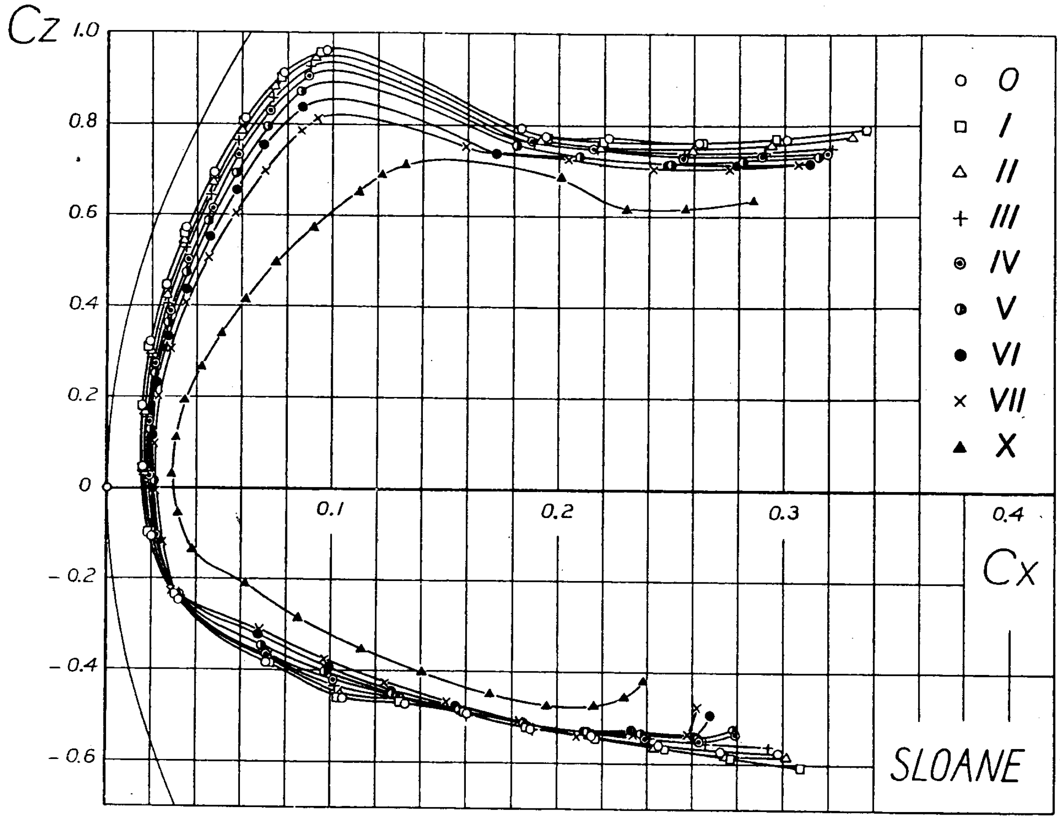


Fig. 50. Polar curves.

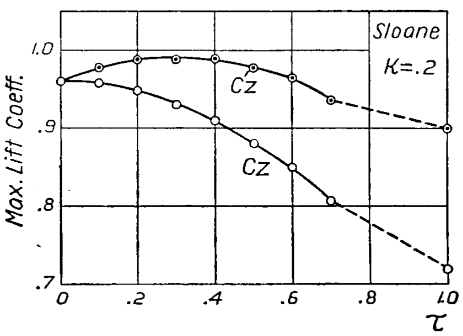


Fig. 51. Variation of the maximum lift coefficient due to the depth of cut-out. Cz′ denotes the value based on the actual wing area.

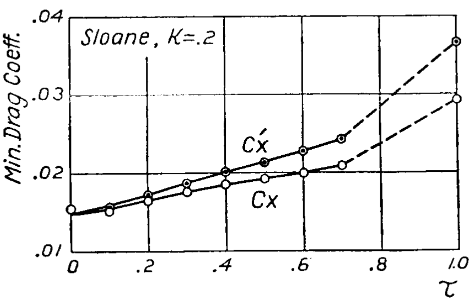


Fig. 52. Variation of the minimum drag coefficient due to the depth of cut-out. Cx′ denotes the value based on the actual wing area.

(ii) *Drag coefficient.* Fig. 46 shows the variation of the drag coefficient due to the depth of cut-out. The curves of the aerofoils from 0 to VII intersect each other at $\alpha = +5^\circ$ and $-6^\circ$. At the angles between $\alpha = -6^\circ$ and $+5^\circ$ the drag coefficient increases with the depth. The minimum drag coefficient increases as the depth of cut-out increases, as is shown in Fig. 52.

The polar curves shown in Fig. 50 indicate that the profile drag increases exceedingly with the depth while the induced drag increases slightly only when the depth becomes considerably large.

(iii) *Moment coefficient and centre of pressure coefficient.* The moment coefficient decreases as the depth of cut-out increases, as is shown in Fig. 47. Decrease of the centre of pressure coefficient with the depth is not so much as that due to the width, as is shown in Fig. 48.

(iv) *Lift/drag ratio.* The curves of the lift/drag ratio are shown in Fig. 49. The maximum value of this ratio decreases as the depth increases, but the values after stall are seen to be independent to the cut-out.

## 5. Summary of the results and conclusions.

(i) *Lift coefficient.* The general variation of the lift coefficient due to cut-outs for any wing section is decrease of the slope of the lift curve. Denoting $\frac{dc_z}{d\alpha}$ of the original aerofoil and the aerofoil with cut-outs by $\bar{c}$ and $c$ respectively, the results of the tests of the Göttingen 593 and 459 wings can be expressed by the following equation for $\tau < 0{\cdot}5$ and all values of $k$.

$$\frac{c}{\bar{c}} = 1 - 1{\cdot}217\,\tau^2 k\,(2-k).$$

The variation of zero lift angle due to cut-out is shown in Fig. 53. In the case of a wing of symmetrical profile like Göttingen 459 wing, the angle of incidence for zero lift is not affected with cut-out, but for wing of cambered profile as Göttingen 593 and Sloane wings it decreases due to cut-out. However, the angle for zero lift of the aerofoil with the cut-out extended the full chord depth is the same as that of the original aerofoil in spite of having the cambered profile.

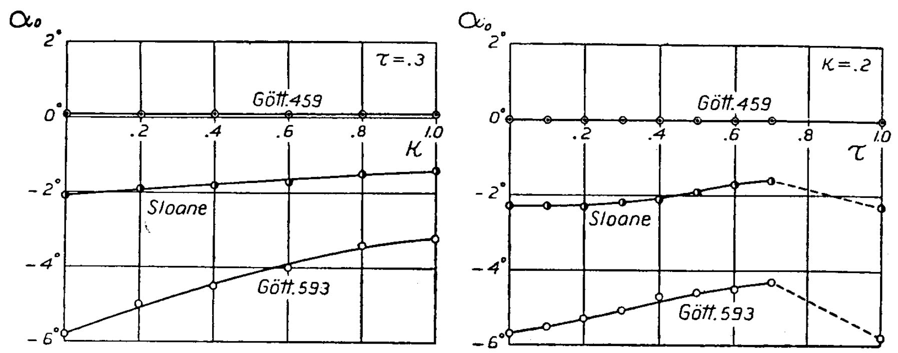


Fig. 53. Variation of zero lift angle due to cut-out.

It thus presents the information that for the symmetrical profiles the decrease of the lift coefficient due to cut-out is only the magnitude corresponding to the decrease of the value of $dc_z/da$ but for the cambered profiles it is added by the magnitude corresponding to the decrease of zero lift angle.

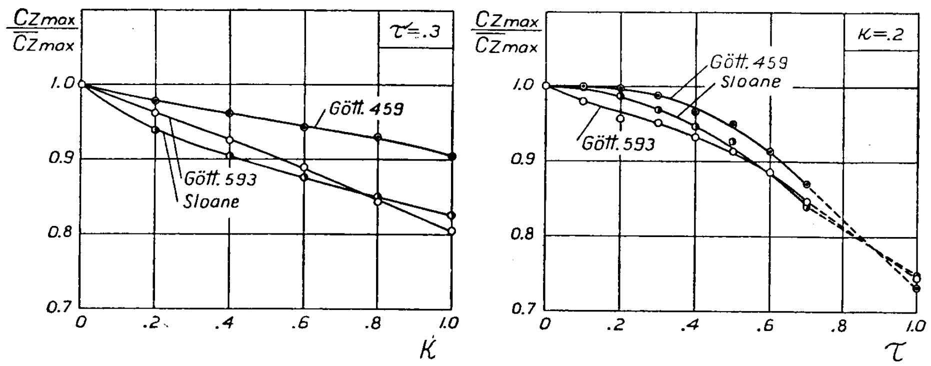


Fig. 54. Variation of the maximum lift coefficient due to cut-out.

Fig. 54 shows the variation of the maximum lift coefficient due to cut-out. The rate of decrease for symmetrical profiles is smaller than that for cambered profiles.

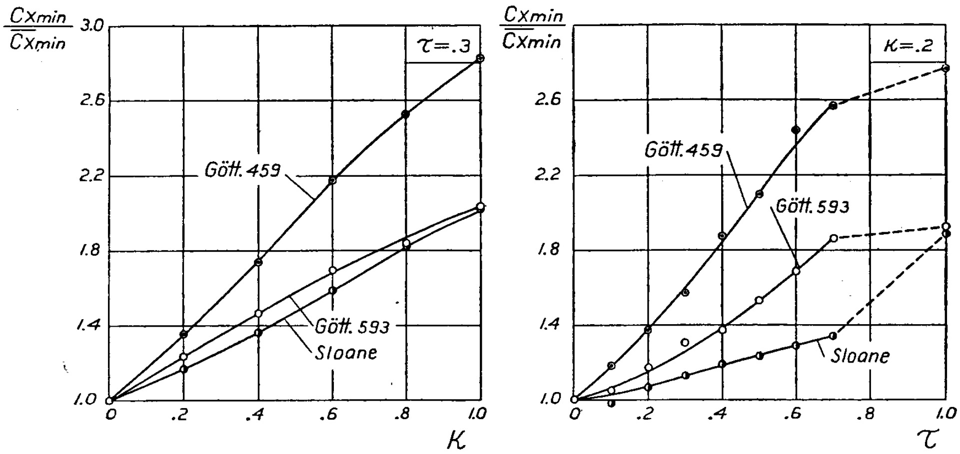


Fig. 55. Variation of the minimum drag coefficient due to cut-out.

(ii) *Drag coefficient.* The most noticeable change in the drag coefficient due to cut-out at rear portion of the wing is the increase of the profile drag. The induced drag seems to be not so affected by such a cut-out except when the depth of cut-out is considerably large.

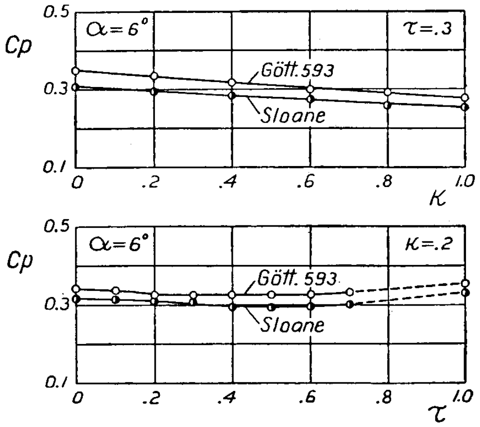


Fig. 56. Variation of the centre of pressure coefficient due to cut-out.

The rate of increase of the minimum drag coefficient due to cut-out for the symmetrical profile Göttingen 459 is greater than that for the other, as is shown in Fig. 55.

(iii) *Moment coefficient and centre of pressure coefficient.* The moment about the leading edge decreases as the cut-out is extended. Fig. 56 shows the variation of the centre of pressure coefficient of the Göttingen 593 and Sloane wings at angle of incidence = +6°. The position of the centre of pressure moves forwards in a linear relation with the width. When the cut-out is extended in the direction of the chord, it moves slightly forwards until $\tau = 0{\cdot}5$ and passing over $\tau = 0{\cdot}5$, it moves conversely backwards.

(iv) *Lift/drag ratio.* The lift/drag ratio decreases in general as the cut-out is extended, but at angles of incidence after stall it seems to be independent to the cut-out. Fig. 57 shows the variation of the maximum value of this ratio due to the cut-out.

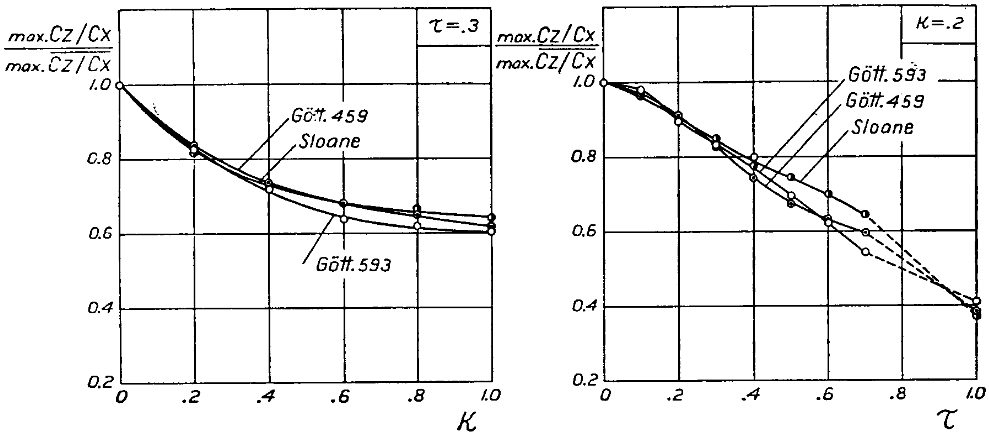


Fig. 57. Variation of the maximum lift/drag ratio due to cut-out.

The results of further experiments and theoretical investigation will be published in another time.

In conclusion the author wishes to acknowledge his best thanks to Prof. Dr. K. Wada for his cordinal guidance and to Mr. T. Fukui for his labour in assisting experiments.

The Wind Tunnel Department,
The Aeronautical Research Institute,
Tokyo Imperial University.
July, 1934.